Theory of fine-structure effects in thermal collisions of $3p$-excited sodium atoms: Combined quasiclassical approximation

I. Yu. Yurova*
Institute of Physics, University of St. Petersburg, St. Petersburg 198904, Russia
(Received 22 June 2001; revised manuscript received 3 December 2001; published 1 March 2002)

Thermal energy collisions of two p-excited alkali-metal atoms have been examined, taking into consideration the fine-structure splitting of atomic energy levels. Collisional-induced transitions between fine-structure levels and energy-pooling processes have been investigated by means of combined semiclassical approximation (CSA). The operator of evolution was constructed with the aid of a numerical solution of a time-dependent quantum electronic equation with appropriate asymptotic Hamiltonian and single trajectory approximation for nuclear motion at large internuclear separations R. Generalized multichannel Landau-Zener model with adiabatic phase averaging for small R has been included in CSA. Numerical results for cross sections in case of scattering of two $3p$-excited sodium atoms in a collision energy range of 300–2000 K have been obtained. The estimation of results accuracy was carried out. The propensity rule for detailed collisional-induced fine-structure transitions has been established.

DOI: 10.1103/PhysRevA.65.032726 PACS number(s): 34.10.+x, 34.20.Cf, 34.50.Fa

I. INTRODUCTION

The energy-pooling processes in thermal collisional energy range in most of the experimental and theoretical works have been considered without a resolution of atomic fine structure

$$A(n_a p)+B(n_b p)\rightarrow A(n_0 l_0)+B(n_f l_f), \tag{1}$$

where $n_0 l_0$ is the ground state of the atom. By means of modern experimental techniques one can populate separate groups of fine-structure levels of colliding atoms (see, for example, reviews [1,2]). The energy-pooling reaction with resolved atomic fine structure could be written as

$$A(np\alpha_1)+A(np\alpha_2)\rightarrow A(n_0 l_0\alpha_0)+A(n_f l_f\alpha_f); \tag{2}$$

here all α_i, α_f are quantum numbers detailed in the fine structure. There are different possible sets of quantum numbers for descriptions of initial and final states, for example, the L picture and the J picture [3], corresponding to ls and jj schemes of electronic structure in atoms. Sometimes, for light atoms especially, it is difficult to define what picture is more suitable in practice [3,4]. Because the J picture was applied rather than the L one in most of the recent experiments (see references below), we apply the J picture. However, the present approach allows us to transform consideration from one picture to another (Sec. III B 2). If atomic fine structure is not distinguished in the final state, instead of Eq. (2) we have

$$A(np_{j_1})+A(np_{j_2})\rightarrow A(n_0 l_0)+A(n_f l_f). \tag{3}$$

Cross section of the process (3) is equal to the average over projections m_1, m_2 of total electronic momenta j_1, j_2 of separated atoms in the initial state

$$\sigma_{j_1 j_2,\ n_f l_f}=\frac{1}{(2j_1+1)(2j_2+1)}\times\sum_{m_1=-j_1}^{j_1}\sum_{m_2=-j_2}^{j_2}\sigma_{j_1 m_1 j_2 m_2,\ n_f l_f}, \tag{4}$$

where $\sigma_{j_1 m_1 j_2 m_2,\ n_f l_f}$ are energy-pooling cross sections of processes with fixed initial values of momenta projections

$$A(np,j_1 m_1)+B(np,j_2 m_2)\rightarrow A(n_0 l_0)+B(n_f l_f). \tag{5}$$

Besides energy pooling the fine-structure effects in thermal scattering of excited atoms are collision-induced fine-structure transitions

$$A(np_{j_1})+A(np_{j_2})\rightarrow A(np_{j_1'})+A(np_{j_2'}). \tag{6}$$

The cross section of this process is calculated as the average over initial projections and the sum over final projections of total momenta of detailed cross sections

$$\sigma_{j_1 j_2,\ j_1' j_2'}=\frac{1}{(2j_1+1)(2j_2+1)}\times\sum_{m_1=-j_1}^{j_1}\sum_{m_2=-j_2}^{j_2}\sum_{m_1'=-j_1'}^{j_1'}\sum_{m_2'=-j_2'}^{j_2'}\times\sigma_{j_1 m_1 j_2 m_2,\ j_1' m_1' j_2' m_2'}, \tag{7}$$

where $\sigma_{j_1 m_1 j_2 m_2,\ j_1' m_1' j_2' m_2'}$ are cross sections of detailed processes

$$A(np,j_1 m_1)+A(np,j_2 m_2)\rightarrow A(np_{j_1' m_1'})+A(np_{j_2' m_2'}). \tag{8}$$

The influence of initial polarization of excited atoms on energy-pooling processes has been investigated mostly in experiments with excited alkali-metal atoms: $3p_{j_1}-3p_{j_2}$ (Na)

*E-mail address: Inna.Yurova@pobox.spbu.ru

[5], $3p$, m_1-3p, m_2 (Na) [4], $4p_j-4p_j$ (K) [6], $6p_j-6p_j$ (Cs) [7,8]; $5s-nl$ (Rb) [9]. In the experiment [3] the dependence of probability of associative ionization on initial polarization of $3p$-excited atoms Na was considered. Besides alkali-metal atoms, the process (3) has been investigated in collisions with excited alkaline-earth-metal targets: Ca [10,11], Sr [12,13], Ba [14–16]. Moreover, there are experiments with excited atoms of other kinds: Cd [17], In [18], and Yt [19] with the observation of the reaction (3).

Despite the great number of experiments [3–19], there are only a few theoretical works dealing with fine-structure effects in the field of thermal collisions of neutral excited atoms: in [20,21] the energy pooling in sodium has been considered. Approaches developed in [20,21] did not take into account the spin-orbit splitting of atomic energy levels or the interaction between colliding atoms at large internuclear distances. That is why methods [20,21] could hardly be applied to the problem of interest without any generalization.

In the present paper, the choice of the proper approximation is considered in Sec. II. The basic equations are presented in Sec. III. Average phase approximation and formulas for cross sections are presented in Sec. IV. The details of numerical calculations are described in Sec. V. The results for cross sections of processes (6), (8), (3), and (5) with propensity rules for fine-structure transitions and discussions are presented in Sec. VI and concluding remarks are presented in Sec. VII.

II. CHOICE OF APPROXIMATION

There are well-known theoretical approaches: quantum, quasiclassical, and classical. Let us consider the purely quantum approach: it could be applied in the very low-collision temperature range (not exceeding 1 K), when hyperfine-structure effects are exhibited (see review [2]). In the thermal energy range the purely quantum approach to the problem of nuclear motion needs to include a prohibitively large number of partial waves $N_{\rm nuc}$. For example, in the case of sodium-sodium collisions at $E_{\rm coll}=100$ K the $N_{\rm nuc}$ is estimated as about 350 and more for higher energies. Above, the complicated electronic part of the problem has to be solved: for *np-np* atom-atom collision the minimum number of two-atomic orbitals in the interval of large internuclear separations R is equal to 36, for small R the basis set is 1000 times more. So one needs to solve minimum $36\times 350=12\,600$ close-coupling equations at large R only in one energy point. Keeping in mind about 50–100 points for formation of the energy dependences of cross sections we need a minimum of 10^6 coupling differential equations of second order, the number is too large even for modern computer devices.

The advantages of classical trajectory approximation can be seen straightforwardly: if a trajectory is known, one is required to solve only 36 coupled first-order time-dependent differential equations for electronic *np-np* functions at large R. On the other hand, the well-developed single trajectory formalism for nuclear motion under thermal energies breaks down in the interval of small internuclear distances, where the interaction between nuclei is considerably large, and causes the splitting of the single trajectory to a number of adiabatic quasimolecular potential curves (for example, see the review [22]).

The quasiclassical approach to nuclear motion seems to be the most suitable one at small R, but it needs to be joined with classical description at large R, because there are no calculations of adiabatic curves there. Thus, we combine in the present paper the quantum nonstationary approach for the electronic problem and classical trajectory approximation for nuclear motion at large R with the quasiclassical method of nonadiabatic transitions at small R. For these purposes the space of relative internuclear distance is divided into two zones: the *inner* zone of small R: $R<R_{\rm mat}$ and the *outer* zone of large R: $R>R_{\rm mat}$ (see Refs. [21], [23], [24], and [25]). The $R_{\rm mat}$ is the boundary point or the matching radius. Thus three basic assumptions (i–iii) could be formulated as follows:

(i) In the outer region $R>R_{\rm mat}$ the nuclear motion can be considered as the classical one and fixed trajectory formalism could be applied there. From comparative estimations of the value of atom-atom interaction, the energy of spin-orbit splitting, and the value of thermal collision energy $E_{\rm coll}$, one can assume the validity of straight trajectory approximation [21], neglect the change of the value of relative velocity v during the collision in the outer region, and put $v=v_{\rm coll}$. The equation of the straight trajectory is well known,

$$R(t)=\sqrt{\rho^2+v^2t^2}, \tag{9}$$

where, ρ is the impact parameter.

(ii) We believe that in the outer region the energy differences between states from $(npnp)$ and other manifolds $(n_1l_1n_2l_2)$ are large in comparison with $E_{\rm coll}$, so one can neglect transitions between different manifolds there. This assumption is valid for $(3p3p)$ manifold of the Na_2 system for example, but it fails in the case of system $Cs(6p)+Cs(6p)$, where manifolds $(6s6d)$ and $(6p6p)$ take approximately the same energy interval [28].

(iii) In the inner region, transitions between states by the same molecular symmetry from $3p3p$ and other manifolds $(3s5s,\ 3s4d,\ 3s4f)$ [26] take place, and they are induced by nonadiabatic interaction in small intervals ΔR_n centered at points $R=R_n$ of pseudocrossings (PCs) between adiabatic molecular curves [24]. The size of intervals ΔR_n should be considerably less than the distances between the nearest PCs: $\Delta R_n \ll |R_n-R_{n\pm1}|$; correspondent estimations are shown in Sec. 5.2 of Ref. [21]. Within intervals ΔR_n we assume the validity of the approximation of constant local radial velocity of nuclear motion $v_{{\rm rad},\alpha}$ (see formula (7) in Ref. [26]), thus a suitable exactly solvable model (presently, the Landau-Zener one) of nonadiabatic transitions could be applied there. Outside of intervals ΔR_n nuclear motion can be considered as the quasiclassical one along adiabatic potential curves. We belive that these curves can suitably be described within the molecular scheme Hund's case (a) [29].

According to the assumption (iii) the conservation of energy of nuclear motion in the inner zone at impact parameter ρ at points R, neglecting small intervals of PCs localizations ΔR_n, could be written by formula

$$E_{\rm coll}=\frac{\mu}{2}v_{{\rm rad},\alpha}^2+\frac{\mu}{2R^2}\rho^2+U_\alpha(R),\quad E_{\rm coll}=\mu v_{\rm coll}^2/2, \tag{10}$$

where μ is the reduced mass of the system, $v_{{\rm rad},\alpha}$ is the radial velocity of relative nuclear motion on the curve α with potential energy $U_\alpha(R)$, and $v_{\rm coll}$ is the initial relative collision velocity of nuclei.

We combine all assumptions (i)–(iii) under the name *Combined Quasiclassical Approximation* (CQA). According to assumptions (i) and (iii) cross sections in CQA can be calculated in impact parameter approximation [27]

$$\sigma_{\gamma\gamma'}=2\pi\left(\frac{E_{\gamma'}}{E_\gamma}\right)^{1/2}\int_0^\infty P_{\gamma\gamma'}\rho d\rho, \tag{11}$$

where E_γ and $E_{\gamma'}$ are energies of initial and final states, $P_{\gamma\gamma'}$ is the probability of transition between states γ and γ', and ρ is the impact parameter.

By analogy with Ref. [21] we define the boundary between the inner and outer regions as $R_{\rm mat}=\rho_{\rm max}$, where $\rho_{\rm max}$ is the maximum impact parameter for penetration of the two-atomic system into the inner region: in other words, at impact parameters $\rho>\rho_{\rm max}$ the system cannot reach any pseudocrossing (PC). From energy conservation (10) we have $\rho_{\rm max}=\max\{R_n[1-U_\alpha(R_n)/E_{\rm coll}]\}$, where the maximum had to be found over all PCs "n" in the inner region. The dependence of $\rho_{\rm max}$ on $E_{\rm coll}$ is shown in Fig. 1 of Ref. [21]. For the system of two $3p$-excited sodium atoms we have $\rho_{\rm max}=46-28a_0$ at collision energies 300–2000 K. Note, that we do not take into account ion-valence PCs with large R_n, such as PC $6^1\Sigma_g^+-7^1\Sigma_g^+$ localized at $R_n=57a_0$ (see Fig. 1(a) in Ref. [26]); ion-valence PCs could be important in the case of ionization processes [22]). We applied the set of sodium-sodium adiabatic curves from the configuration interaction (CI) calculations and Landau-Zener parameters of PCs from Ref. [26] with a correction of the misprint in parameter $2V_n$ of PC 1 (d) in Table I in [26] from 1.80×10^{-5} to 1.80×10^{-4}. Along with the letter set, we applied another set of Landau-Zener parameters (see Sec. VI A).

Interval of validity of CQA

In the case of the $(3p3p)$ system of two isolated sodium atoms the maximum energy difference between fine-structure components, $2[E(3p_{3/2})-E(3p_{1/2})]$, is equal to 49.4 K [28], so one can establish the lower limit of the validity of assumption (i) as $E_{\rm coll}\gtrsim200-300$ K. One can determine the upper collisional energy limit of the validity of the present approximation from the position of the highest quasimolecular curve and we can also take into consideration the model approach for the inner region.

The highest curve obtained in the last work was the $(3s4f)$ curve: the next upper curve should be the $(3s5p)$ one. If collision energy exceeds the threshold of excitation of the $(3s5p)$ state, the model approach requires more quasimolecular curves than is computed now, so we can estimate the upper energy limit as the excitation energy of the $(3s5p)$ state, that is about 2000 K, so we have: $E_{\rm coll}\lesssim2000$ K. Thus, combining the latter estimations, we establish the collision energies range of the validity of the present approximation

$$300\ {\rm K}\lesssim E_{\rm coll}\lesssim2000\ {\rm K}. \tag{12}$$

III. BASIC EQUATIONS

A. Coordinate frames

The classical relative motion of two nuclei in the outer region is described by the frame with the origin in the center of mass of two nuclei and, with axes **X**, **Y**, **Z**, are parallel to these by laboratory frame. The axis **Z** is directed along the vector of initial relative collision velocity. This frame is named as the frame center of mass with laboratory axes (FCMD). The collisional plane in FCML is the plane **YZ**. The azimuthal angle φ in the plane **YZ** defines the direction of internuclear axis.

In the inner region we apply the molecular frame (FM) with the origin in the center of mass, the axis **Xm**, that coincides with **X**, and the axis **Zm**, directed along the vector of internuclear separation **R**. In the initial state of collision, two frames FCML and FM coincide. As nuclei move relative to each other, the plane **Ym Zm** in FM rotates together with the internuclear axis relative to the plane **YZ** in FCML.

The choice of coordinate frames reflects the application of different approaches to the description of nuclear motion in the outer and inner zones [27]. As nuclei are far from each other, FCML is more suitable for application of single trajectory approximation than the FM one [see assumption (i) in Sec. II]. For small internuclear separations FM seems more suitable for the quasimolecular approach [see assumption (iii) in Sec. II].

B. Asymptotic Hamiltonian and operator of evolution

The method of asymptotic Hamiltonian was applied in Ref. [34] in the case of $Na(3p)+Na(3p)$ slow collisions and in [32,33] in the case of Rb+Rb* thermal collisions. We cannot apply unchanged Hamiltonians proposed in letter references because, in the case of Rb+Rb* interaction [33], the dipole-dipole operator dominates in the Coulomb part of the interaction; on the other hand, the asymptotic Hamiltonian, proposed in [34], contains the quadrupole-quadrupole operator, but the Coriolis term was not included in it because of its smallness for too small collision velocities, considered in [34]. We construct the asymptotic Hamiltonian $\mathbf{H}_{\rm as}$, combining expressions from [33,34]

$$\mathbf{H}_{\rm as}=\mathbf{H}_1+\mathbf{H}_2+\mathbf{V}_{\rm Cor}+\mathbf{V}_{12}.$$

$\mathbf{H}_1$, $\mathbf{H}_2$ are effective Hamiltonians of valence electrons in separate atoms, $\mathbf{V}_{\rm Cor}$ is the Coriolis operator, and $\mathbf{V}_{12}$ is the operator of interaction between colliding atoms.

1. $3p3p$ subspace of electronic wave functions

In order to construct the matrix of asymptotic Hamiltonian (13) in the outer region, one needs to apply a suitable basis set for electronic wave function. According to assump-

tion (i) from Sec. II we expect that there are no transitions in the outer region between $3p3p$ and $3s5s$, and $3s4d$ and $3s4f$ electronic configurations of the Na+Na system

$$(\mathbf{H}_{\rm as})_{\beta\gamma}=0; \quad |\beta\rangle \in (3s5s,\ 3s4d,\ 3s4f), \quad |\gamma\rangle \in (3p3p). \tag{13}$$

From properties (13) it follows that it is sufficient to construct the matrix of asymptotic Hamiltonian only in $3p3p$ subspace. The two-electrons asymptotic $3p3p$ basis set can be composed from different products of spin-orbitals ϕ_{m,m_s} of separated atoms

$$\phi_{m,\ m_s}(\mathbf{r},\sigma)=R_{3p}(r)Y_{1m}(\hat{r})\chi_{m_s}(\sigma), \quad m=-1,0,1;\ \ m_s=\pm 1/2. \tag{14}$$

Here, Y_{1m} is the spherical function and χ_{m_s} is one-electron spin function.

2. Representations for electronic wave functions

In order to apply any pictures (L or J, see Sec. I) for a description of electronic states in the outer region, and also to construct the matrix of asymptotic Hamiltonian, one needs to apply different representations for electronic wave functions: *ls*, *jj*, and *MA*. Note that *ls* representation is equivalent to the L picture, *jj* to the J picture. In any representation two-electronic two-center basis functions should be antisymmetric versus the permutation of the spatial and spin coordinates of two electrons. In the present paragraph we consider different representations in the $(3p3p)$ subspace.

ls representation. Two-electron two-center antisymmetric basis functions with orbital momenta of electrons $l_1=l_2=1$, their projections m_{l1}, m_{l2}, and projections of spins $(m_{s1},m_{s2}=\pm 1/2)$ can be written as

$$|m_{l1}m_{s1},m_{l2}m_{s2}\rangle=\frac{1}{\sqrt{2}}(1-\mathbf{P}_{12}) \times[\phi_{m_1,m_{s1}}(\mathbf{r}_1,\sigma_1)\phi_{m_2,m_{s2}}(\mathbf{r}_2,\sigma_2)]. \tag{15}$$

$\mathbf{P}_{12}$ is the operator of the permutation of all coordinates of electrons 1 and 2; $\phi_{m_1,m_{s1}}$ and the $\phi_{m_2,m_{s2}}$ are one-electron (14).

jj representation. *jj* functions can be obtained by transformation from the *ls* basis set with unitary matrix $\mathbf{T}^{(jj-ls)}$

$$|j_1m_1,j_2m_2\rangle=\sum\ T^{jj\text{-}ls}_{j_1m_1j_2m_2,m_{l1}m_{s1}m_{l2}m_{s2}}|m_{l1}m_{s1},\ m_{l2}m_{s2}\rangle, \tag{16}$$

$$T^{jj-ls}_{j_1m_1j_2m_2,m_{l1}m_{s1}m_{l2}m_{s2}}=C^{j_1m_1}_{1m_{l1}\frac{1}{2}m_{s1}}C^{j_2m_2}_{1m_{l2}\frac{1}{2}m_{s2}},$$

where $C^{j_im_i}_{1m_{li}1/2m_{si}}$, $i=1,2$ are the Clebsh-Gordan coefficients [35]. The labeling of the *jj* basis functions is given in Table I.

TABLE I. Labeling of two-electrons *pp*-basis functions in *jj* representation.

N	j_1	m_{j1}	j_2	m_{j2}	N	j_1	m_{j1}	j_2	m_{j2}
1	3/2	3/2	3/2	3/2	19	3/2	−1/2	3/2	3/2
2	3/2	3/2	3/2	1/2	20	3/2	−1/2	3/2	1/2
3	3/2	3/2	1/2	1/2	21	3/2	−1/2	1/2	1/2
4	3/2	3/2	3/2	−1/2	22	3/2	−1/2	3/2	−1/2
5	3/2	3/2	1/2	−1/2	23	3/2	−1/2	1/2	−1/2
6	3/2	3/2	3/2	−3/2	24	3/2	−1/2	3/2	−3/2
7	3/2	1/2	3/2	3/2	25	1/2	−1/2	3/2	3/2
8	3/2	1/2	3/2	1/2	26	1/2	−1/2	3/2	1/2
9	3/2	1/2	1/2	1/2	27	1/2	−1/2	1/2	1/2
10	3/2	1/2	3/2	−1/2	28	1/2	−1/2	3/2	−1/2
11	3/2	1/2	1/2	−1/2	29	1/2	−1/2	1/2	−1/2
12	3/2	1/2	3/2	−3/2	30	1/2	−1/2	3/2	−3/2
13	1/2	1/2	3/2	3/2	31	3/2	−3/2	3/2	3/2
14	1/2	1/2	3/2	1/2	32	3/2	−3/2	3/2	1/2
15	1/2	1/2	1/2	1/2	33	3/2	−3/2	1/2	1/2
16	1/2	1/2	3/2	−1/2	34	3/2	−3/2	3/2	−1/2
17	1/2	1/2	1/2	−1/2	35	3/2	−3/2	1/2	−1/2
18	1/2	1/2	3/2	−3/2	36	3/2	−3/2	3/2	−3/2

MA representation. In this molecular representation by Hund's case (a), L and S, the total electronic orbital and spin momenta, can be expected as good quantum numbers. *MA* wave functions can be obtained from the *ls* ones by the unitary transformation with the matrix $\mathbf{M}^{MA\text{-}ls}$:

$$|w\Lambda SM_S\rangle=\sum\ M^{MA\text{-}ls}_{w\Lambda SM_S,m_{l1}m_{s1}m_{l2}m_{s2}}|m_{l1},m_{s1},\ m_{l2}m_{s2}\rangle, \tag{17}$$

where w is the parity, Λ is the module of the total orbital momentum projection, S and M_S are the total spin and its projection of the two-atomic system, $|m_{l1}m_{s1},\ m_{l2}m_{s2}\rangle$ are two-electrons two-center orbital from the *ls* representation. The matrix of $M^{(MA\text{-}ls)}$ can be found by the application of symmetrization operators to the *ls* basis functions (for example, see formulas (3.2.1) and (3.2.2) in Ref. [21]) and then with hybridization in $\Sigma(\sigma\sigma)-\Sigma(\pi\pi)$ subspace in order to get the diagonal form of quadrupole-quadrupole operator [39]. Note that molecular basis functions without hybridization coincide with these from Table I in Ref. [34]).

3. Matrix of asymptotic Hamiltonian in 3p3p subspace

Let us consider the construction of separate terms in the asymptotic Hamiltonian (13).

Effective operators of valence electrons in separate atoms. We assume as in Ref. [33] that these operators are diagonal in *jj* representation

$$\mathbf{H}_{i,j_1m_1j_2m_2}=E_{j_i}\delta_{m_1,m_2}, \quad i=1,2, \tag{18}$$

where E_{j_i} are energies of electronic states of isolated atoms including spin-orbit splitting E_{so}; one can find E_{j_i} and E_{so} in tables [28]. We expect also, as it was done in Ref. [33] for

the Rb+Rb system, that the value of spin-orbital splitting in the two-atomic system is not changed significantly in the interval $\infty > R > 15a_0$ at least.

From the expressions for Coriolis operator in Refs. [30,31,36,24], we have

$$\mathbf{V}_{\mathrm{Cor}} = -\frac{\partial \varphi}{\partial t}\hat{J}_x, \quad \hat{J}_x = \hat{J}_{1x} + \hat{J}_{2x}, \tag{19}$$

where φ is the angle of rotation around the the vector of the total nuclear orbital momentum J, which is directed along the axis **X** (see Sec. III A), $\hat{J}_x$ is the operator of the rotation of space and spin coordinates of electrons around the axis **X**, and $\hat{J}_{1x}$ and $\hat{J}_{2x}$ are operators of the projections on the axis **X** of the total electronic momenta of separate atoms. The classical description of nuclear motion in the molecular frame assumes the proportionality of Coriolis operator $\mathbf{V}_{\mathrm{Cor}}$ to the angular velocity of nuclei $\partial\varphi/\partial t$ in the frame FCML, that can be found from the equation of the trajectory (9)

$$\frac{\partial \varphi}{\partial t} = -\frac{\rho v}{R^2}. \tag{20}$$

With the aid of expressions (19), (9), and (20), and applying the quantum expression for matrix elements of operator of x projection of total electronic momentum of atom i $\hat{J}_{ix}$ [37], we can write

$$(\mathbf{V}_{\mathrm{Cor}})_{j_1 m_1 j_2 m_2} = \frac{\rho v}{R^2}\langle m_1|\hat{J}_{1x}|m_1'\rangle \times \langle m_2|\hat{J}_{2x}|m_2'\rangle \delta_{j_1 j_1'}\delta_{j_2 j_2'}\delta_{m_1 m_1' \pm 1}\delta_{m_2 m_2' \pm 1},$$

$$\langle m_i|\hat{J}_{1x}|m_i - 1\rangle = \langle m_i - 1|\hat{J}_{1x}|m_i\rangle = \frac{1}{2}\sqrt{(j_i + m_i)(j_i - m_i + 1)}, \quad i = 1,2. \tag{21}$$

In the outer region the Coulomb part of interatomic interaction $\mathbf{V}_{12}$ can be represented in the form of a series expansion in powers of $1/R$ [38], the first two components in it in the case of two identical atoms being in the same electronic states are the quadrupole-quadrupole and the second-order dipole-dipole terms; adding the exchange part we have for $\mathbf{V}_{12}$ the expression

$$\mathbf{V}_{12} = -\mathbf{V}_{\mathrm{qq}}/R^5 - \mathbf{V}_6/R^6 + \mathbf{V}_{\mathrm{ex}}, \tag{22}$$

where $\mathbf{V}_{\mathrm{qq}}$, $\mathbf{V}_6$, and $\mathbf{V}_{\mathrm{ex}}$ are quadrupole-quadrupole, second-order dipole-dipole and exchange operators.

Quadrupole-quadrupole interaction. $\mathbf{V}_{\mathrm{qq}}$ between two identical p-excited atoms has been constructed in the *ls* representation [39]

TABLE II. Eigenvalues of operator $\mathbf{V}_{qq}$ for Na($3p$)+Na($3p$) system.

MA-state[a]	Ref. [34]	Ref. [40]	Ref. [41]	Present
$^1\Delta_g, ^3\Delta_u$	−365	−554	−381	−367
$^1\Pi_g, ^3\Pi_u$	1460	2220	1526	1468
$^1\Pi_u, ^3\Pi_g$	0	0	0	0
$^1\Sigma_u^+, ^3\Sigma_g^+$	0	0	0	0
$h1\,^1\Sigma_g^+, h1\,^3\Sigma_u^+$[b]	[c]	−3325[d]	−2289	−2202
$h2\,^1\Sigma_g^+, h2\,^3\Sigma_u^+$[b]	[c]	0[d]	0	0

[a]In *MA* representation the operator $\mathbf{V}_{qq}$ has diagonal form.
[b]Labels $h1$ and $h2$ mean different states $^1\Sigma_g^+$ and $^3\Sigma_u^+$, constructed from $3p(\sigma)$ and $3p(\pi)$ atomic orbitals by hybridization in order to diagonalize $\mathbf{V}_{qq}$ (*iu* and *il* states in Ref. [26], corresponding to upper and lower adiabatic potential curves).
[c]See text in Sec. III B 3.
[d]The value is obtained by the diagonalization of the matrix C_5 from Ref. [40].

$$(\mathbf{V}_{\mathrm{qq}})_{\alpha,\beta} = \sum_{\mu=-2}^{2} \frac{(-1)^\mu 4!}{(2+|\mu|!)^2}(Q_2^\mu)_{m1,m2}(Q_2^\mu)_{m1',m2'}\delta_{m_{s1}} \times m_{s1'}\delta_{m_{s2},\ m_{s2'}}, \tag{23}$$

$$(Q_2^\mu)_{m1,\ m2} = \langle r^2\rangle\langle m_1|Y_2^\mu|m_2\rangle.$$

Here $\alpha = |m_1 m_{s1} m_2 m_{s2}\rangle$ and $|\beta\rangle = |m_1' m_{s1}' m_2' m_{s2'}\rangle$ are two-electronic states with $l_1 = l_2 = 1$; Y_2^μ are spherical functions; quadrupole operator of the isolated atom with one effective p electron, $(Q_2^\mu)_{m1',m2'}$, one can find in Table III of Ref. [39] and Table II of Ref. [34]. It is seen from formula (23), that values of all matrix elements of operator $\mathbf{V}_{\mathrm{qq}}$ can be expressed via the single parameter $\langle r^2\rangle$—the mean square radius of the valence electron in the $3p$-excited state of isolated atom.

We transformed operator $\mathbf{V}_{\mathrm{qq}}$ (23) from *ls* into the *MA* representation by means of formulas (16) and (17). The matrix of $\mathbf{V}_{\mathrm{qq}}$ is diagonal in the *MA* basis set and with accuracy to a value of the multiplier $\langle r^2\rangle$ coincides with matrices C_5 from Table II in Ref. [41] and from Table IV in Ref. [40] (see Table II in present paper). Note that in Ref. [34] they apparently did not account for the existence of the non diagonal $\Sigma(\sigma\sigma) - \Sigma(\pi\pi)$ matrix elements of the operator $\mathbf{V}_{\mathrm{qq}}$ in the molecular representation without hybridization. Note also, that in Ref. [42] actually the quadrupole-quadrupole matrix elements have been considered and applied in the *ls* representation instead of the *MA* one (see Table I in Ref. [42]).

Applying the one-electron model potential for the calculation of the $3p$ wave function, we estimated the value of the $\langle r^2\rangle$ as $39.2-39.5a_0^2$. This value is close to what ($39a_0^2$) has been estimated in Ref. [42] by the method of Bates and Damgaard [43], but differs from the $54.6a_0^2$, calculated in Ref. [40] by the variation-perturbation method, and from the $46.92a_0^2$, calculated in Ref. [44] by the multiconfiguration

TABLE III. Matrix elements of $\mathbf{V}_6$ for $\mathrm{Na}(3p)+\mathrm{Na}(3p)$ system in *MA* representation.

Molecular state	Ref. [40][a]	Ref. [47]	Ref. [45][a]	Ref. [41]
$^1\Delta_g, ^3\Delta_u$	2600	6303	1560	2509
$^1\Pi_g, ^3\Pi_u$	−500	9134	3830	5431
$^1\Pi_u, ^3\Pi_g$	1010	9134	2940	1910
$^1\Sigma_u^+, ^3\Sigma_g^+$	−500	7550	4310	4270
$h1^1\Sigma_g^+, h1^3\Sigma_a^{+}$[b]	2000	1460	3410	1816
$h2^1\Sigma_g^+, h2^3\Sigma_u^{+}$[b]	20200	−7550	4310	−397

[a]Nondiagonal matrix elements are not shown.
[b]See notations of states in Table II.

Hartree-Fock method. Perhaps the last discrepancy can be explained by the correlation energy effect, which appeared in calculations [44].

The operator of *second-order dipole-dipole interaction* is given by formulas (17) and (28) in the review [38]. In the paper [45] the simple analytical expression for matrix elements of dipole-dipole interaction in the *jj* representation has been obtained, according to Ref. [45], the matrix $\mathbf{V}_6$ in the sum (22) has the diagonal form

$$
\begin{aligned}
(\mathbf{V}_6)_{\alpha,\beta}=\Bigg[& -C_{\mathrm{ss}}+C_{\mathrm{aa}}\frac{m_1m_2(3\cos^2\vartheta-2)}{12j_1j_2} \\
& +\Bigg\{ C_{\mathrm{ts}}\frac{3m_1^2-j_1(j_1+1)}{2j_1(2j_1-1)} \\
& +C_{\mathrm{st}}\frac{3m_2^2-j_2(j_2+1)}{2j_2(2j_2-1)}\Bigg\}\frac{3\cos^2\vartheta-1}{2} \\
& +3C_{\mathrm{tt}}\frac{3m_1^2-j_1(j_1+1)}{2j_1(2j_1-1)} \\
& \times\frac{3m_2^2-j_2(j_2+1)}{2j_2(2j_2-1)}\,\frac{9\cos^4\vartheta-8\cos^2\vartheta+1}{2}\Bigg] \\
& \times\delta_{j_1j_2'}\delta_{j_2j_2'}\delta_{m_1m_1'}\delta_{m_2m_2'}; \qquad (24)
\end{aligned}
$$

$$
\alpha=|j_1m_1j_2m_2\rangle,\quad \beta=|j_1'm_1'j_2'm_2'\rangle.
$$

Values of constants in the formula (24) in the case of two $3p$-excited sodium atoms have been calculated in Ref. [45]

$$
C_{\mathrm{ss}}=3040,\ C_{\mathrm{aa}}=-7420,\ C_{\mathrm{st}}=C_{\mathrm{ts}}=331,\ C_{\mathrm{tt}}=-1050.
$$

Besides Ref. [45] other calculations of operator $\hat{V}_6$ have been made. Opposite to Ref. [45], where the matrix of $\mathbf{V}_6$ is diagonal in the *jj* representation, in Refs. [40–42,47] the matrix of $\mathbf{V}_6$ is diagonal in *MA* or the *ls* representation, in Ref. [34] the matrix of $\mathbf{V}_6$ is diagonal in *MA* except $\sigma\sigma$-$\pi\pi$ matrix elements in Σ subspace. The matrix (24) was transformed into the *MA* basis set in the present paper. Values of diagonal matrix elements $\mathbf{V}_6$ are presented in Table III. One can see that there is significant disagreement in values and in signs between different sets of results for operator $\mathbf{V}_6$. Fortunately, the inclusion of the operator $\mathbf{V}_6$ into the present calculations almost does not change the results for cross sections because of the smallness of matrix elements of $\mathbf{V}_6$ in comparison with the quadrupole-quadrupole and Coriolis matrix elements in the outer region, and we do not apply the operator $\mathbf{V}_6$ any more (see Sec. V).

Exchange interaction $\mathbf{V}_{\mathrm{ex}}$. In Ref. [46] matrices of asymptotic exchange interaction in the *ls* representation for n_1sn_2s, n_1sn_2p and n_1pn_2p excited states of two interacting atoms were derived in analytical expressions, see Table 4.3 of the Ref. [24]. Matrix of exchange interaction in the case of $3p3p$ states of sodium atoms, is constructed by means of formula (4.76–4.77) from Ref. [24], it can be written as

$$
\begin{aligned}
\mathbf{V}_{\mathrm{ex}}=0.4326A^4R^{5.407}(R\mathbf{V}_{\mathrm{ex},1}+\mathbf{V}_{\mathrm{ex}2}+\mathbf{V}_{\mathrm{ex}3}/R) \\
\times\exp(-0.945\,R),
\end{aligned}
$$

where $\mathbf{V}_{\mathrm{ex},i}$, $i=1,2,3$ are constant matrices, A is the coefficient in asymptotic expression for the one-electron radial $3p$ function of sodium atom for large electron-nucleus separation r: $R_{3p}(r)=\mathrm{Ar}^{4.5}\exp(-0.472r)$. We estimated the value of parameter A as $A=0.159$ by means of the effective one-electron potential method. Exchange interaction decreases exponentially while $R\to\infty$ being induced by overlap of atomic wave functions located on different centers. The estimation of matrix elements $\mathbf{V}_{\mathrm{ex}}$ (25) shows, that at internuclear distances $R>R_{\mathrm{mat}}$, where $R_{\mathrm{mat}}=27-29a_0$ (outer region) one can neglect by exchange interaction in comparison with quadrupole-quadrupole and Coriolis one.

Gathering expressions (18)–(22), one can obtain asymptotic Hamiltonian for the system $\mathrm{Na}(3p)+\mathrm{Na}(3p)$. Dependences on internuclear distance R of eigenvalues of asymptotic Hamiltonian (13) for two cases of Coriolis interaction have been obtained [Figs. 1(a) and 1(b)]. It is seen, that asymptotic interaction cannot mix states with different sums of total momenta j_1+j_2 at the outer zone, also the interaction does not cause new PCs between curves in Fig. 1 when Coriolis interaction raises. These features are displayed in results for cross sections of collisional-induced fine-structure transitions (Sec. VI).

C. Operator of evolution U^{out} in outer region

According to the assumption (ii) from Sec. II and equalities (13), values of matrix elements of operator U^{out} between $(3p3p)$ and other subspaces, could be put equal to zero

$$
U^{\mathrm{out}}_{\beta\beta'}=\delta_{\beta\beta'};\quad U^{\mathrm{out}}_{\gamma\beta}=0;
$$

$$
|\beta\rangle,|\beta'\rangle\in(3s5s,\quad 3s4d,\ 3s4f),\quad |\gamma\rangle\in(3p3p). \qquad (25)
$$

The dimension of functional space where the operator $\mathbf{U}^{\mathrm{out}}$ should be defined, is equal to 86, the number is summed from dimensions 2, 36, 20, and 28 of subspaces $(3s5s)$, $(3p3p)$, $(3s4d)$, and $(3s4f)$, respectively. In fact, equalities (25) give an opportunity to calculate only the restricted

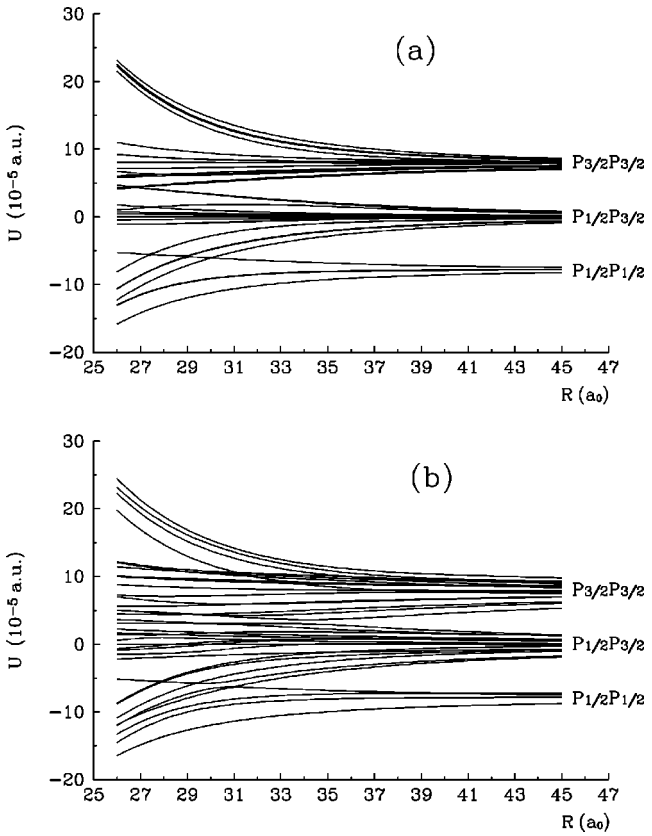

FIG. 1. Eigenvalues of asymptotic Hamiltonian (13) in $3p3p$ subspace for two sodium atoms for collision energy $E_{\rm coll}=1000$ K and two values of impact parameter: (a) $\rho=5a_0$; (b) $\rho=27a_0$.

operator $U^{\rm out}$ on the subspace $3p3p$ with the dimension equal to 36. Matrix elements of $U^{\rm out}$ are defined by expressions

$$U^{\rm out}_{\alpha,\alpha'}(-\infty,-t_{\rm mat})=\langle\Psi_\alpha(-t_{\rm mat})|\alpha'\rangle,\quad |\alpha\rangle,|\alpha'\rangle\in 3p3p, \tag{26}$$

where $-t_{\rm mat}$ is the moment of time, when system reaches the boundary of the inner region, moving from $t=-\infty$, from Eq. (9) one has $t_{\rm mat}=v/\sqrt{R^2_{\rm mat}-\rho^2}$, functions Ψ_α are solutions of the nonstationary Schröedinger matrix equation

$$i\frac{\partial}{\partial t}\Psi_\alpha(t)=\sum_{\alpha''}(\mathbf{H}_{\rm as})_{\alpha,\alpha''}\Psi_{\alpha''}(t). \tag{27}$$

Initial conditions for Eq. (27) are

$$|\Psi_\alpha(-\infty)\rangle=|\alpha\rangle,\quad |\alpha\rangle\in(3p3p). \tag{28}$$

Here $|\alpha\rangle$ are $3p3p$ basis functions, they could be written in any representation: *ls*, *jj*, or *MA*; the connection between different representations is established by formulas (15)–(17).

In order to obtain the solution of Eq. (27) one needs to begin the numerical procedure from infinitely large t or R. Really one begins the procedure from sufficiently large definite values, that demands computational time. These wastes could be escaped by the application of the analytical method of *rotational transformation*. We introduce a distance $R_{\rm Cor}>R_{\rm mat}$ by the condition, that for $R>R_{\rm Cor}$ Coriolis interaction becomes much larger than other components of asymptotic Hamiltonian (27)

$$(\mathbf{V}_{\rm qq})_{ik}+(\mathbf{V}_6)_{ik}\ll(\mathbf{V}_{\rm Cor})_{ik},\quad i,k=1,36;\quad R_{\rm Cor}<R. \tag{29}$$

One can see from formula (19), that the Coriolis term is the infinitesimal operator in respect to the rotation in the space of electronic functions around the axis **X**, which is perpendicular to the collisional plane (Sec. III A). Bearing in mind, that matrices of energies of isolated atoms commute with the matrix of Coriolis interaction, the solution of Eq. (27) in the zone $R>R_{\rm Cor}$ can be expressed via matrix **Y** of the rotational transformation

$$\Psi_{j_1m_1,\ j_2m_2}(-t_{\rm Cor})=\sum_{j_1'm_1'j_2'm_2'}Y_{j_1m_1j_2m_2,\ j_1'm_1'j_2'm_2'}\Psi_{j_1'm_1'j_2'm_2'}(-t_{\rm Cor}),$$

$$\mathbf{Y}_{j_1m_1j_2m_2,j_1'm_1'j_2'm_2'}=D^{j_1}_{m_im_1'}(\alpha,\ \beta,\ \gamma)\times D^{j_2}_{m_2m_2'}(\alpha,\ \beta,\ \gamma)\delta_{j_1j_1'}\delta_{j_2j_2'}, \tag{30}$$

where $D^j_{mm'}$ are Wigner *D*-functions (Ref. [35]) with arguments: $\alpha=\pi/2$, $\beta=\arcsin(-\rho/R_{\rm Cor})$, and $\gamma=\pi/2$. With the aid of transformation (30) we can restrict numerical procedure of Eq. (27) by substitution in initial conditions (28) the infinity by definite value of $t_{\rm Cor}$ that could be found from the value of $R_{\rm Cor}$ [see condition (29) and the equation of trajectory (9)]. Thus for the operator of evolution we have

$$\mathbf{U}^{\rm out}(-\infty,-t_{\rm mat})=\mathbf{Y}\cdot\mathbf{U}^{\rm out}(-t_{\rm Cor},-t_{\rm mat}). \tag{31}$$

It is useful to establish the *symmetry properties* of the operator $\mathbf{U}^{\rm out}$ following from the identity of colliding atoms and from the symmetry against the time inversion

$$\mathbf{U}^{\rm out}_{j_1m_1,j_2m_2,j_1'm_1'j_2'm_2'}=\mathbf{U}^{\rm out}_{j_2m_2j_1m_1,j_2'm_2'j_1'm_1'}$$

$$\mathbf{U}^{\rm out}_{j_1m_1j_2m_2,j_1'm_1'j_2'm_2'}=i^{(j_1+j_2+j_1'+j_2')}\mathbf{U}^{\rm out}_{j_1-m_1j_2-m_2j_1'-m_1'j_2'-m_2'}. \tag{32}$$

D. Operator of nonadiabatic transitions $U^{\rm in}$ in inner region

The asymptotic Hamiltonian (13) is not valid in the inner region, and moreover, the single trajectory approximation for nuclear motion breaks there [see assumptions (i)–(iii) in Sec. II]. In analogy with the operator of evolution $\mathbf{U}^{\rm out}$, we can construct the model operator $\mathbf{U}^{\rm in}$, that transforms the electronic wave function as a result of passing by the two-atomic system the inner zone from one boundary point $\mathbf{R}^-_{\rm mat}$ to another one $\mathbf{R}^+_{\rm mat}$, for given impact parameter and collision energy

$$\Psi(\mathbf{R}^+_{\rm mat})=\mathbf{U}^{\rm in}\Psi(\mathbf{R}^-_{\rm mat}). \tag{33}$$

Points $\mathbf{R}^{+}_{\rm mat}$ are defined by the same internuclear distance $R_{\rm mat}$ but different angles $\varphi\pm$ in collisional plane (see Sec. III A). The dimension of the matrix of the operator $\mathbf{U}^{\rm in}$ is the same as the $\mathbf{U}^{\rm out}$ one; properties (25) are not valid for the operator $\mathbf{U}^{\rm in}$ [see assumption (iii) in Sec. II], but there are other properties of matrix elements of $\mathbf{U}^{\rm in}$, presented below.

In order to find the operator $\mathbf{U}^{\rm in}$ we apply the generalized method of nonadiabatic transitions, combining formulas from Refs. [26], [24], and [36]. Let the number of PCs in the inner zone equal n_m and the unitary transition matrices $\hat{N}(n)$, $n=1,...,n_m$, transform adiabatic electronic functions $\alpha\rangle$ and $\beta\rangle$ after passing of the single separate PC n between curves α and β, located at the point $R=R_n$

$$(\hat{N}(n))_{\alpha,\beta}=-(\hat{N}(n))^{*}_{\beta;\alpha}=\sqrt{P_n}e^{i\sigma_n},\quad \alpha\neq\beta;$$

$$(\hat{N}(n))_{\alpha\ \alpha}=(\hat{N}(n))^{*}_{\beta,\beta}=e^{-i\phi_n}\sqrt{1-P_n};$$

$$(\hat{N}(n))_{\gamma,\gamma'}=\delta_{\gamma,\gamma'},\quad \gamma,\ \gamma'\neq\alpha,\ \beta. \tag{34}$$

Parameters P_n, ϕ_n and σ_n of the matrix $\hat{N}_n$ (34) can be found with the aid of any suitable exactly solvable model of two states [24]. In the case of the Landau-Zener model $\sigma_n=0$, P_n is the Landau-Zener probability of the transition, the value of $\phi\leqslant\pi/4$ [24].

Let diagonal matrices $\hat{A}(R_n,R_{n+1})$ transform adiabatic wave functions according to the assumption (iii) of Sec. II: after passing by the system of the interval between adjacent PCs, located at points R_n and R_{n+1}, functions get phase multipliers in accordance with the quasiclassical approach

$$\hat{A}_{\alpha,\ \alpha'}(R_n,\ R_{n+1})=\exp(i\phi_{n,n+1}),$$

$$\phi_{n,\ n+1}=\int_{R_n}^{R_{n+1}}k_\alpha(R)dR\,\delta_{\alpha,\alpha'},\quad n=1,\ldots,n_m. \tag{35}$$

From the equality (10) we find the $k_\alpha(R)=\sqrt{2\mu[E_{\rm coll}(1-\rho^2/R^2)+U_\alpha(R)]}$ is the classical impulse of the radial nuclear motion along adiabatic curve $'_{\alpha'}$. The transition operator in the inner region can be written with accuracy to real phase c as the product of matrices defined by formulas (34) and (35) [24]

$$U^{\rm in}=\exp(ic)\mathbf{U}^{\rm in}_{1/2}(\mathbf{U}^{\rm in}_{1/2})^{\rm tr},$$

$$\mathbf{U}^{\rm in}_{1/2}=\hat{A}(R_{\rm mat},R_1)\hat{N}_1\hat{A}(R_1,R_2)\hat{N}_2\cdots\hat{A}(R_{n_m,\ n_{m+1}})\hat{N}_{n_m}. \tag{36}$$

Note, that in formulas (35) and (36) under the point of R_{n_m+1} the turning point on curves α are assumed. According to the assumption (iii) from Sec. II we apply the scheme Hund's *a* in the inner region, the following properties of the operator $\mathbf{U}^{\rm in}$ could be expressed by equalities:

$$(\mathbf{U}^{\rm in})_{\alpha,M_{S,\ i},\ \alpha,M_{S,\ k}}=u_\alpha\delta_{M_{S,\ i},\ M_{S,\ k}},$$

$$(\mathbf{U}^{\rm in})_{\gamma,+\Lambda}=(\mathbf{U}^{\rm in})_{\gamma,-\Lambda}, \tag{37}$$

where the first property is written for multiplet states, value of u_α does not depend on projections of total spin M_{S_i}, M_{S_k}, and α means all quantum numbers of the given state except of M_S. The second property is written for states with $\Lambda\neq0$.

IV. CROSS SECTIONS AND AVERAGING OVER ADIABATIC PHASES

We calculate cross sections with the aid of formula (11), where both states $|\gamma\rangle$, $|\gamma'\rangle\in(3p3p)$ in the case of the fine-structure transition (8); in the case of the energy-pooling process (5) $|\gamma'\rangle$ is the final state $3snl$.

The transition probability $P_{\gamma,\gamma'}$ can be calculated as a matrix element of a product of operators

$$P_{\gamma,\ \gamma'}=\left|[\mathbf{U}^{\rm out}\cdot\mathbf{T}^{jj-MA}\cdot\mathbf{U}^{\rm in}\cdot(\mathbf{U}^{\rm out}\cdot\mathbf{T}^{jj-MA,{\rm tr}}]_{\gamma,\gamma'}\right|^2. \tag{38}$$

Here the operator $\mathbf{U}^{\rm out}$ is defined by formulas (25)–(32), the operator $\mathbf{U}^{\rm in}$ by Eq. (36), the matrix $\mathbf{T}^{(jj-MA)}=\mathbf{T}^{(jj-ls)}\cdot(\mathbf{T}^{(MA-ls)})^{\rm tr}$ connects representation *jj* with *MA* one (see formulas (16) and (17). $\mathbf{T}^{(jj-MA)}$ is applied here, because the operator $\mathbf{U}^{\rm out}$ is constructed in *jj* representation due to the definition of initial states in the *J* picture (Sec. I), and the operator $\mathbf{U}^{\rm in}$ in the *MA* one due to the scheme of Hund's *a*, adopted in the inner region. Matrix elements of the operator $\mathbf{U}^{\rm in}$ (36) contain adiabatic phases $\phi^{(m)}_{\rm ad}$ (35) as arguments of functions $\sin[\phi^{(m)}_{\rm ad}]$ and $\cos[\phi^{(m)}_{\rm ad}]$. One can expect, that these functions change rapidly with the variation of ρ under the thermal collision energies, and after the integration over the impact parameter in the formula for cross section (11) with transition probability from Eq. (38), all terms with oscillating multipliers become considerably small and one could neglect them. This approximation we call by *phase averaging*; it can be written as the equality

$$P_{\gamma,\gamma'}=\sum_{\alpha\ \beta}|\mathbf{U}^{\rm out}_{\gamma,\ \alpha}|^2\mathbf{P}^{\rm in}_{\alpha,\ \beta}|(\mathbf{U}^{\rm out})^{\rm tr}_{\beta,\ \gamma'}|^2, \tag{39}$$

where the matrix $\mathbf{P}^{\rm in}$ can be obtained as the product of probability matrices from single PC $\mathbf{P}(m)$

$$\mathbf{P}^{\rm in}=\mathbf{P}(1)\mathbf{P}(2)\cdot\mathbf{P}(n_m)\mathbf{P}(n_m)\cdots\mathbf{P}(1). \tag{40}$$

Matrix elements of matrices $\mathbf{P}(n)$, $n=1,\cdots,n_m$ are equal to square modules of elements of single transition matrices $\hat{N}(n)$ (34): $\mathbf{P}(n)_{\alpha,\beta}=|[\hat{N}(n)]_{\alpha,\alpha}|^2$. Note that nonzero matrix elements of $\mathbf{P}^{\rm in}$ (40) are equal to elements, these have been calculated in Ref. [26].

From consideration given in the present section, it follows, that after averaging over adiabatic phases it is sufficient to find values of transition probabilities through single PC instead of complex matrix elements of matrices $\hat{N}(n)$ (34). We proved the validity of the phase averaging approximation for sodium-sodium thermal collisions by numerical calculations of the energy-pooling cross section without phase averaging and with it, considering the motion along curves by $^1\Sigma^+_g$ symmetry. Results of calculations showed

that cross sections calculated with phase averaging and without it differ maximum at 6% for $E_{\rm coll}=300$ K; then as collision energy grew up to 2000 K, the maximum difference between results decreased up to 2%. Thus deviation is not large and one can believe, that the validity of phase averaging is proved. Note, that calculations without phase averaging demand much more computer time, than with application of phase averaging approximation.

Taking into account expressions (11) and (38), in adiabatic average phase approximation the expression for the cross section could be written as

$$\sigma_{\gamma\gamma'}=2\pi\left(\frac{E_{\gamma'}}{E_\gamma}\right)^{1/2}\int_0^{R_{\rm mat}}\sum_{\alpha,\beta}|[\mathbf{U}^{\rm out}\cdot\mathbf{T}^{\mathbf{jj-MA}}]_{\gamma\alpha}|^2\mathbf{P}^{\rm in}_{\alpha\beta}\times|[(\mathbf{T}^{(jj-MA)})^{\rm tr}(\mathbf{U}^{\rm out})^{\rm tr}]_{\beta\gamma'}|^2\rho d\rho+2\pi\left(\frac{E_1}{E_2}\right)^{1/2}\int_{R_{\rm mat}}^{\infty}|[\mathbf{U}^{\rm out}\cdot(\mathbf{U}^{\rm out})^{\rm tr}]_{\gamma\gamma'}|^2\rho d\rho. \quad (41)$$

The second integral in the sum (41) does not contain the matrix $\mathbf{P}^{\rm in}$, because it is calculated over the outer region, where there are no transitions between states from the $3p3p$ manifold and from other ones ($3s5s$, $3s4d$, and $3s4f$) there [see assumption (ii) in Sec. II].

V. CALCULATIONS

In order to check our calculations with formula (41) we controlled the conservation of unitary properties of the operator $\mathbf{U}^{\rm out}$ on different steps of calculation procedure, also we solved Eq. (27) in both *jj* and *MA* representations and obtained the same results. The rotational transformations (31) and symmetry properties (32) allowed us to reduce the time of numerical calculations, also they reduce the number of independent detailed cross sections of processes (8) from 1296 to 432.

Calculations of the matrix elements of the matrix $\mathbf{P}_{\rm in}$ (40) were made with the aid of a program from Ref. [26]. The value of $R_{\rm Cor}$ in formula (29) has been chosen in the interval $110-120a_0$; the amplifying of this value did not change results more than on 0.1%.

Calculations were made with two different choices of the operator $\mathbf{V}_6$: with values from formula (24), and with values from Ref. [47], (see Table III in this paper). Results showed that the cross section is almost independent on the choice of $\mathbf{V}_6$. In practice it is possible to calculate cross sections of fine-structure transitions without the inclusion of the operator $\mathbf{V}_6$ into consideration.

We examined the influence of the exchange interaction $\mathbf{V}_{\rm ex}$ (25) on the results. The calculations showed that the results are not sensitive to the inclusion of the $\mathbf{V}_{\rm ex}$ into the asymptotic Hamiltonian (13).

The property of cross sections relative to inversion of time is expressed by the detailed balance rule [formula (144.13) in Ref. [37]]:

$$\sigma_{\gamma'\gamma}/E_{\gamma'}=\sigma_{\gamma^*\gamma'^*}/E_\gamma, \quad (42)$$

where states γ'^* and γ^* differ from states γ' and γ by the inversion of time, it is equivalent to the inversion of signs of all momenta; $E_\gamma=E_{\rm coll}+E_{j_1j_2}$ and $E_{\gamma'}=E_{\rm coll}+E_{j_1'j_2'}$. It was checked that calculated cross sections satisfy the equality (42) exactly for all collision energies $E_{\rm coll}$ the satisfiability of detailed balance rule confirms the correctness of present calculations.

VI. RESULTS AND DISCUSSIONS

Averaged and detailed cross sections of collisional-induced fine-structure transitions (6) and (8), have been calculated with the aid of formulas (41) and (7). Averaged over projections m_1, m_2 and summed over m_1', m_2' cross sections (6) are presented in Figs. 2(a) and 2(b). The present calculations showed that transition without the change of sum j_i+j_k are less efficient then these with conservation of the sum [Figs. 2(a) and 2(b)]. Also it was noticed, that transitions (6) with the change of the sum j_1+j_2 take place mostly in the inner zone, but transitions with the constant sum j_i+j_k take place mostly in the outer zone. It is seen from Figs. 2(a) and 2(b), that cross sections of inelastic processes with the change of the sum of total electronic momenta of atoms $\Delta(j_1+j_2)=1$ and $\Delta(j_1+j_2)=2$ do not differ from each other considerably in case of transitions $3/23/2\rightarrow 1/21/2$ and $3/21/2\rightarrow 1/21/2$ [curves (2) and (3) in Figs. 2(a) and 2(b)]. The letter could be explained by the symmetry properties of quadrupole-quadrupole operator (23).

Results of calculations of detailed cross sections (8) lead to the *propensity rule: Transitions* $j_1m_1j_2m_2\rightarrow j_1'm_1'j_2'm_2'$ *are the most efficient with* $j_1+j_2=j_1'+j_2'$ or

$$\Delta(j_1+j_2)=0. \quad (43)$$

Taking in mind transitions between states, that are not connected by detailed balance rule (42) and symmetry properties (32), the propensity rule is confirmed in case of the first 122 of the most efficient collisional-induced fine-structure transitions. It follows from present calculations, that their cross sections are almost independent on collision energy at $E_{\rm coll}>900\,^\circ$K. In notations of Table I the first ten of the most efficient transitions are: 17–27, 15–29, 5–25, 3–30, 1–36, 6–10, 11–21, 10–20, 4–19, and 11–16. Energy dependences of cross sections of transitions 15–29, 5–25, and 3–30 relative to the transition 17–27 are presented in Fig. 3(a). The transition 17–27 (1/2 1/2, $1/2-1/2\rightarrow 1/2-1/2$, 1/2 1/2) has the most valued cross section, the correspondent energy dependence is presented in Fig. 3(b). Propensity rule and steady energy dependences of cross sections in case of collisional-induced fine-structure transitions could be explained by the features of eigenvalue curves of asymptotic Hamiltonian [Fig. 1], as it was discussed in Sec. III D. We could not find obvious propensity rule in case of transitions with $\Delta(j_1+j_2)=1$, 2. We noted, that transitions with the maximum value of $(m_1+m_2-m_1'-m_2')$ are more effective in general than other ones nevertheless.

Average cross sections of *energy-pooling transitions* (5) have been calculated by means of formulas (41) and (4). Note, that cross sections in the formula (41) should be

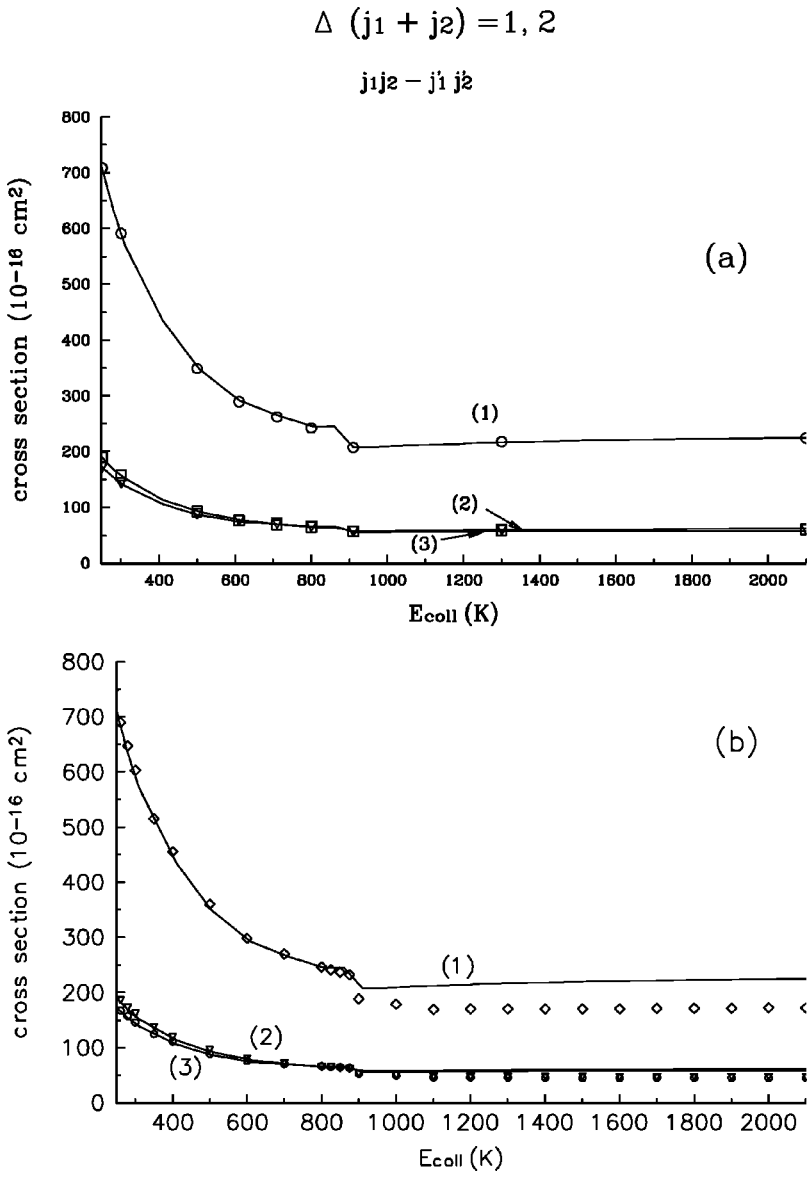

FIG. 2. Energy dependences of averaged cross sections of collisionally induced fine-structure transitions (6) in cases $\Delta(j_1+j_2)=1, 2$: (1) transition 3/2 3/2→3/2 1/2, (2) transition 3/2 3/2→1/2 1/2, (3) transition 3/2 1/2→1/2 1/2. In (a) and (b) lines—calculations with the parameter of quadrupole-quadrupole interaction $\langle r^2\rangle = 39.2a_0^2$ and set I of Landau-Zener parameters of PCs. Circles, squares, and triangles correspond to calculations in cases (1), (2), and (3), with: (a) $\langle r^2\rangle = 46.9a_0^2$ and set I; (b) $\langle r^2\rangle = 39.2a_0^2$ and set II.

summed over over all final fine-structure states for given final quantum numbers $n_0 n_f$; if one takes into account the unitary properties of the operator $\mathbf{U}^{\text{out}}$, the latter summation could be done in *MA* representation over all molecular states γ_f with molecular potential curves having at large internuclear separations the same energy limit $n_0 l_0$, $n_f l_f$ as the energy of the final state in process (5). As a result we have the following expression for cross section:

$$\sigma_{\gamma\gamma'} = 2\pi\left(\frac{E_{\gamma'}}{E_\gamma}\right)^{1/2} \frac{1}{(2j_1+1)(2j_2+1)} \sum_{m_1,m_2} \sum_{\gamma_f} \times \int_0^{R_{\text{mat}}} \sum_\alpha |[\mathbf{U}^{\text{out}} \cdot \mathbf{T}^{\mathbf{jj-MA}}]_{j_1 m_1 j_2 m_2 \alpha}|^2 \cdot \mathbf{P}^{\text{in}}_{\alpha\gamma_f} \rho d\rho;$$

$$\gamma = j_1 j_2, \quad \gamma' = n_0 l_0, \quad n_f l_f. \tag{44}$$

Results for energy-pooling processes have been obtained for three possible pairs of initial total momenta $j_1 j_2$ [Figs. 4(a)–4(c)]. One can see that the energy-pooling cross sections weakly depend on values of $j_1 j_2$.

We could not find any other results except ours about collisional-induced fine-structure transitions, but in the case of energy-pooling processes (3) race constants for different values of (j_1, j_2) at $T = 640\,^\circ$K have been measured (Ref. [5]). In order to compare our results with the data [5] we calculated race constants with the Boltzmann distribution function. One can see from Table IV that the dependence of race constants on values of j_1, j_2, is stronger in Ref. [5] than ours. Also the relative values of race constants of $4F$-state production in Ref. [5] are greater than ours, especially for the case 1/2, 1/2. The discrepancy of theoretical and experimental results could be explained by the too narrow interval of QCA validity for calculation of race constants (see Sec. II), and, on the other hand, by the possible inaccuracy of experimental data. Note that in experiments [4] weak dependence of energy-pooling cross sections on fine-structure quantum numbers in the *ls* picture had been observed.

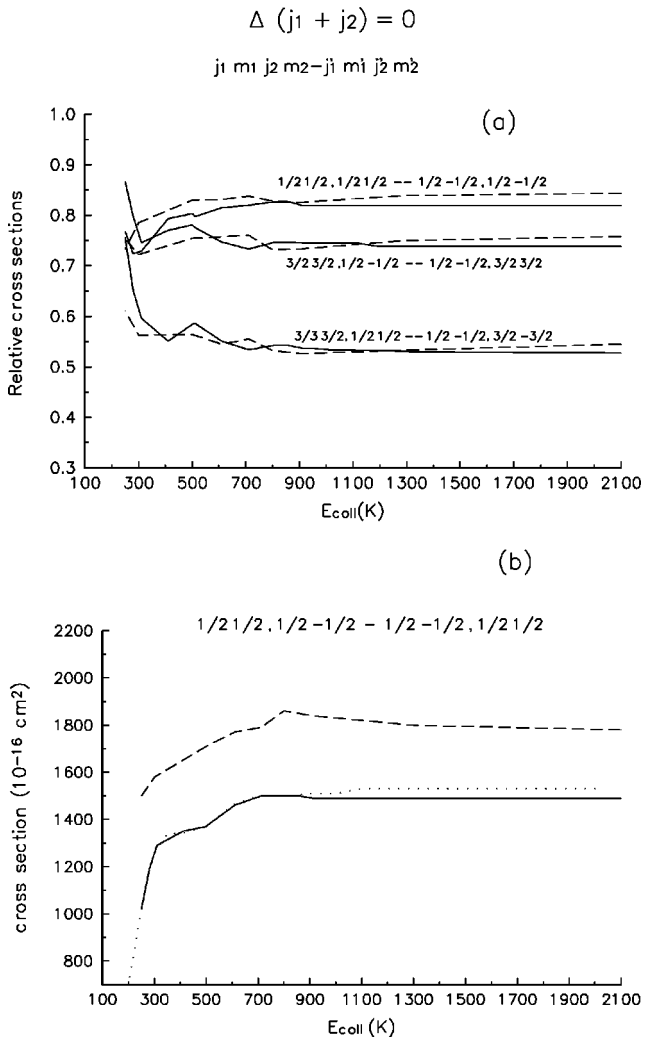

FIG. 3. Energy dependences of cross sections of collision-induced fine-structure are the most efficient transitions (8) in case $\Delta(j_1+j_2)=0$. Solids—calculations with $\langle r^2\rangle=39.2a_0^2$, dashed—with $\langle r^2\rangle=46.9a_0^2$. (a) Cross sections are relative to that of the transition (17–27): 1/2 1/2, 1/2–1/2→1/2–1/2, 1/2 1/2. (b) Cross section of the transition (17–27).

Dependence of results on variation of potential and pseudocrossings parameters

Actually in the present calculations the interatomic interaction in the outer region depends on the single numerical parameter $\langle r^2\rangle$ of the quadrupole-quadrupole term [see formula (23) and the text therein]. Here the $\langle r^2\rangle$ is the mean square radius of a $3p$-valence electron in an excited sodium atom. Cross sections have been calculated with the present value of $\langle r^2\rangle=39.2a_0^2$ and with the value $46.9a_0^2$ from Ref. [44], results are shown in Figs. 2(a), 3(a), 3(b), and 4(a)–4(c). One can notice that these results are weakly sensitive to the variation of $\langle r^2\rangle$ except the absolute values of cross sections in the case of transitions with $\delta(j_1+j_2)=0$ [Fig. 3(b)], where the discrepancy between two sets of results reaches 19%.

In the inner region, instead of application of interatomic interaction, we introduce a set of parameters of Landau-Zener pseudocrossings (PCs). In the present consideration,

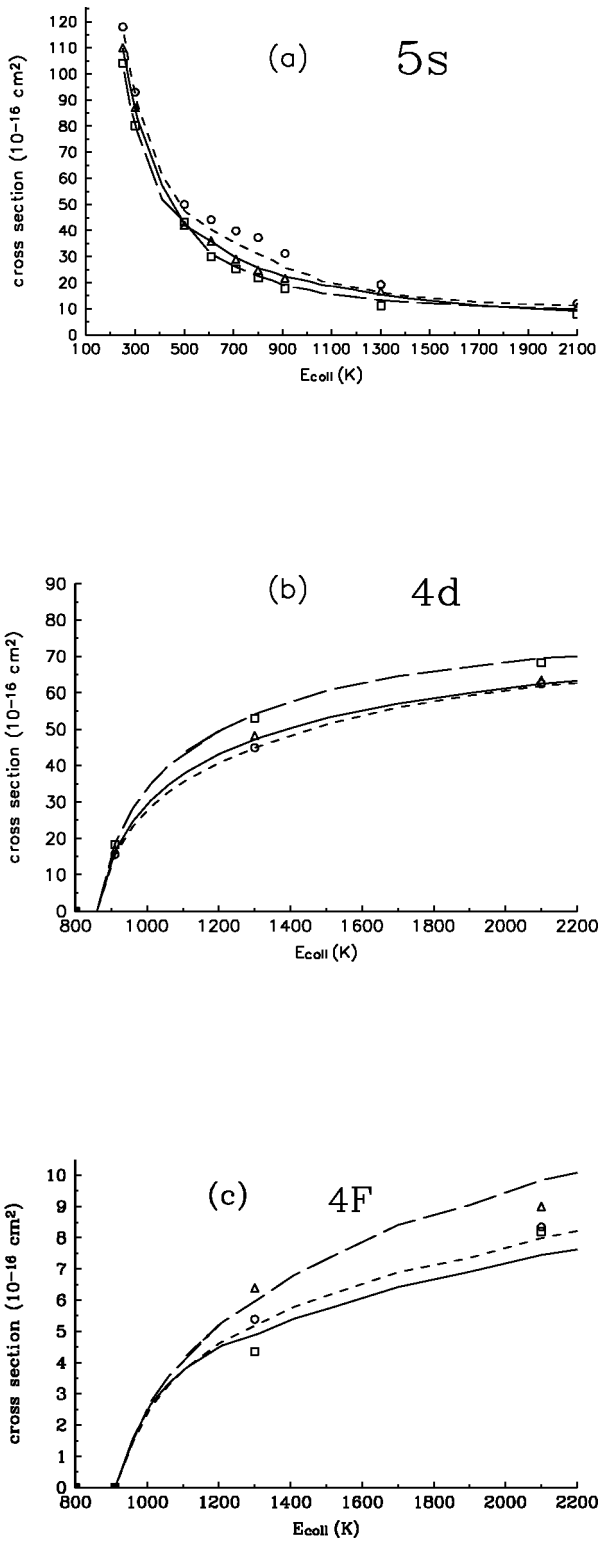

FIG. 4. Energy dependences of averaged over initial projections of total momenta energy-pooling cross sections in case of collisions (6) for three final excited states of sodium atom $n_f l_f=5s$. (a), $4d$ (b), $4f$ (c) and different initial values of total electronic momenta of separate sodium atoms (j_1,j_2): solids and triangles—(3/2, 3/2); long dash and boxes—(3/2, 1/2); short dash and circles—(1/2, 1/2); Lines—calculations with $\langle r^2\rangle=39.2a_0^2$, scatters-with $\langle r^2\rangle=46.9a_0^2$.

TABLE IV. Energy-pooling rate constants ratios $k_{nl}^{j_1,j_2}/k_{5s}^{3/2,3/2}$ at $T=640$ K.

$j_1 j_2$	nl	Present	Ref. [5]
3/2,3/2	4D	2.2	2.2
3/2,3/2	4F	0.23	0.83
1/2,1/2	5S	1.1	3.2
1/2,1/2	4D	2.2	3.2
1/2,1/2	4F	0.24	2.6

we apply two sets of PCs parameters. The set I is given from Ref. [26], the set II includes more thoroughly recalculated values of PCs parameters, with the addition of three PCs by the symmetry $^3\Sigma_u^+$: these PCs had not been mentioned in Ref. [26]. Calculations with sets I and II of PCs parameters have been performed. Statistically averaged over j_1, j_2 initial channels, energy-pooling cross sections computed with set I are in complete agreement with our previous results (Ref. [26]). The comparison of results received with application by two sets of PCs parameters is presented in Fig. 2(b) and Figs. 5(a)–5(c). It is seen from Fig. 2(b), that the most sensitive to the variation of PCs parameters is the cross section of transition 3/2 3/2→3/2 1/2 at $E_{\mathrm{coll}}>900$ K. In the case of energy-pooling processes, the most sensitive to the variation of Landau-Zener parameters is the cross section of $4F$-state production [Fig. 5(c)].

VII. CONCLUDING REMARKS

The present approach CSA combines the quantum description of electrons and the classic approach to nuclear motion. CSA is suitable for practical calculations, as the example, it was applied in the case of thermal collisions of $3p$-excited sodium atoms in the present paper. Three possible representations for electronic wave functions were used, which gives an opportunity to apply as the L picture, and the J picture as well, and to apply both Hund's schemes a and c. The present approach allows us to calculate coherence terms, obtained experimentally by means of coherent population with known density matrix the group of fine-structure states by laser light [3,4]. These calculations have not been made in the present consideration because of the absence of the density matrix that defines the population of atomic initial states, and had to be known from conditions of experiments. The proposed approximation could be applied in cases of excited heavy atoms scattering, in Rb*+Rb* and Cs*+Cs* collisions for example, and could be generalized in case of scattering alkaline-earth-metal atoms.

Note that the present consideration does not allow us to obtain energy-pooling cross sections into final states with detected fine structure, due to the restriction of the basis set in the outer zone by single electronic configuration $3p3p$, and due to the neglect by spin-orbit splitting of adiabatic potential curves in the inner zone.

ACKNOWLEDGMENTS

The author is grateful to Professor V. N. Ostrovsky and Professor H. Nakamura for the helpful discussions and the Institute for Molecular Science (Okazaki, Japan) for their hospitality.

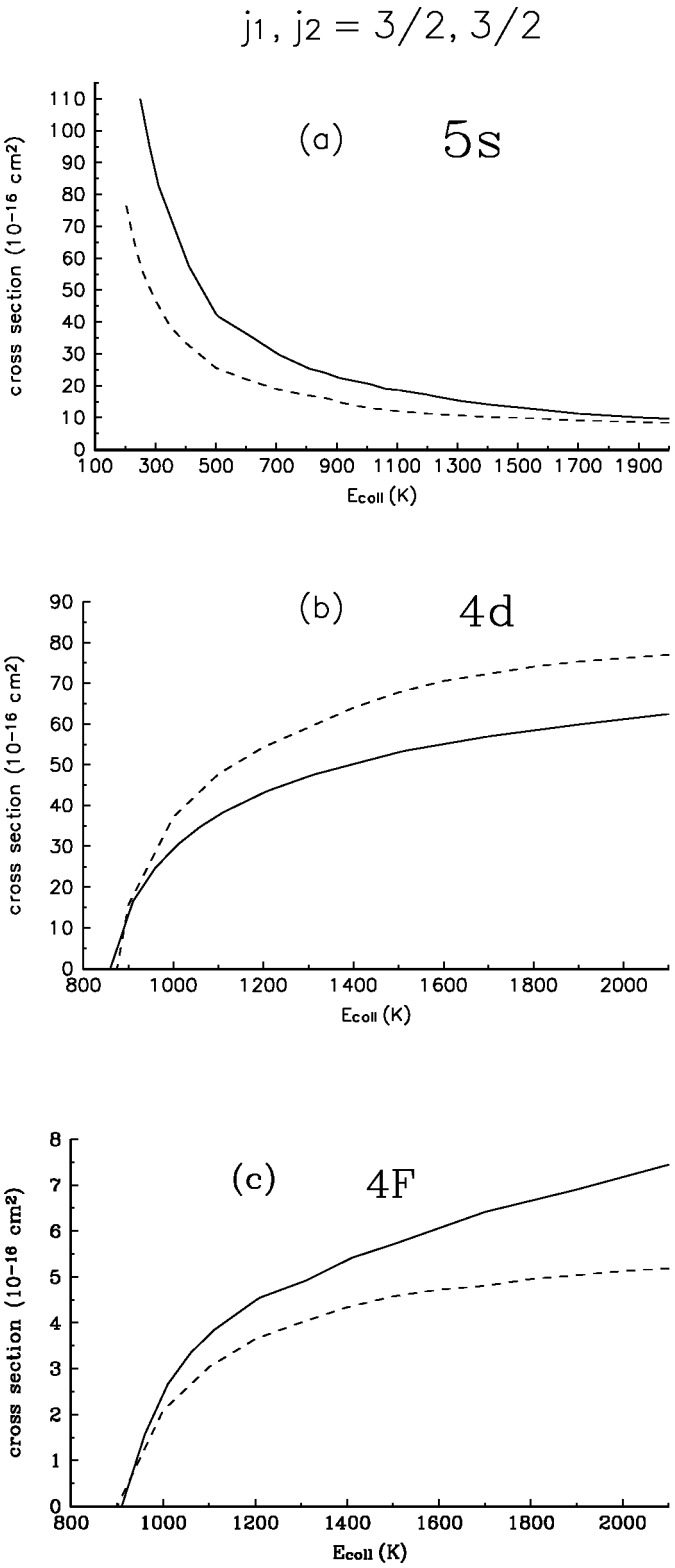

FIG. 5. The same as in Fig. 4 but for the single channel (3/2, 3/2). Solids—calculations with set I of Landau-Zener parameters, dashed—with set II.

[1] N. Andersen, in *The Physics of Electronic and Atomic Collisions*, edited by T. Andersen *et al.*, AIP Conf. Proc. No. 295 (AIP, New York, 1993), p. 505.
[2] P. S. Julienne, A. M. Smith, and K. Burnet, Adv. At., Mol., Opt. Phys. **30**, 141 (1992).
[3] H. A. J. Meijer, T. J. C. Peigrim, and H. J. M. Heideman, J. Chem. Phys. **90**, 738 (1989).
[4] J. H. Nijland, J. A. de Gouw, A. Dijkerman, and H. J. M. Heideman, J. Phys. B **25**, 2841 (1992); J. H. Nijland, J. J. Blange, H. Rudolf, H. A. Dijkerman, and H. J. M. Heideman, *ibid.* **25**, 4835 (1992).
[5] S. A. Davidson, J. F. Kelly, and A. Gallagher, Phys. Rev. A **33**, 3756 (1986).
[6] R. K. Namiotka, J. Huennekens, and M. Allegrini, Phys. Rev. A **56**, 514 (1977).
[7] Z. J. Jabbour, R. K. Namiotka, J. Huennekens, M. Allegrini, M. S. Miloševíc, and F. de Tomasi, Phys. Rev. A **54**, 1372 (1996).
[8] F. de Tomasi, S. Miloševíc, P. Verkerk, A. Fioretti, M. Allegrini, Z. J. Jabbour, and J. Huennekens, J. Phys. B **30**, 4991 (1997).
[9] B. Bieniak, K. Fronc, S. Gateva-Kostova, M. Glodz, V. Grushevsky, J. Klavins, K. Kovalsky, A. Rucinska, and J. Szonert, Phys. Rev. A **62**, 022720 (2000).
[10] H. V. Parks, E. M. Spain, J. E. Smedley, and S. R. Leone, Phys. Rev. A **58**, 2136 (1998).
[11] H. V. Parks and S. R. Leone, Phys. Rev. A **60**, 2944 (1999).
[12] J. A. Nueman, J. Cooper, and A. Gallagher, Phys. Rev. A **56**, 432 (1997).
[13] J. A. Nueman and A. Gallagher, Phys. Rev. A **57**, 2231 (1998).
[14] J. A. Nueman, A. Gallagher, and J. Cooper, Phys. Rev. A **50**, 1292 (1994).
[15] G. de Filippo, S. Guldberg-Kjar, S. Miloševíc, and J. O. P. Pedersen, J. Phys. B **29**, 2033 (1996).
[16] G. de Filippo, D. Romstad, S. Guldberg-Kjar, S. Miloševíc, and J. O. P. Pedersen, Z. Phys. D **39**, 21 (1997).
[17] S. Barsotti, F. Fuso, A. F. Molisch, and M. Allegrini, Phys. Rev. A **57**, 1778 (1998).
[18] P. Bicchi, C. Marinelli, E. Mariotti, M. Meucci, and L. Moi, J. Phys. B **30**, 473 (1997).
[19] C. Gabbanini, A. Lucchesini, S. Gozzini, and L. Moi, Phys. Rev. A **46**, R9 (1992).
[20] P. H. T. Philipsen, J. H. Nijland, H. Rudolf, and H. G. M. Heideman, J. Phys. B **26**, 939 (1993).
[21] I. Yu. Yurova, J. Phys. B **28**, 999 (1995).
[22] R. K. Janev, Adv. At. Mol. Phys. **12**, 1 (1978).
[23] A. F. Wagner and F. K. Parks, J. Chem. Phys. **65**, 4343 (1976).
[24] E. E. Nikitin and S. Ya. Umanskii, *Theory of Slow Atomic Collision* (Springer, Berlin, 1984).
[25] M. Kimura and C. D. Lin, Phys. Rev. A **31**, 590 (1985).
[26] I. Yu. Yurova, O. Dulieu, S. Magnier, F. Masnou-Seeuws, and V. N. Ostrovsky, J. Phys. B **27**, 3659 (1994).
[27] M. S. Child, *Molecular Collision Theory* (Academic, London, 1974), Chap. 8.
[28] C. E. Moore, *Atomic Energy Levels*, Natl. Bur. Stand. (U.S.) Circ. No. 467 (U.S. GPO. Washington, D.C., 1949).
[29] A. Henriet and F. Masnou-Seeuws, J. Phys. B **23**, 219 (1990).
[30] R. T. Pack and J. O. Hirschfelder, J. Chem. Phys. **49**, 4009 (1968).
[31] W. R. Thorson, J. Chem. Phys. **34**, 1744 (1961).
[32] V. Grushevsky, M. Jonsons, and K. Orlovsky, Phys. Scr. **56**, 245 (1997).
[33] K. Orlovsky, V. Grushevsky, and A. Ekers, Eur. Phys. J. D **12**, 133 (2000).
[34] R. W. Heather and P. S. Julienne, Phys. Rev. A **47**, 1887 (1993).
[35] A. R. Edmonds, *Angular Momentum in Quantum Mechanics* (Princeton University, Princeton, NJ, 1957).
[36] H. Nakamura, Phys. Rev. A **26**, 3125 (1982).
[37] L. D. Landau and E. M. Lifshitz, *Quantum Mechanics*, (Pergamon, Oxford, 1965).
[38] A. Dalgarno and W. D. Davison, Adv. At. Mol. Phys. **2**, 1 (1966).
[39] B. Linder and J. O. Hirschfelder, J. Chem. Phys. **28**, 197 (1958).
[40] M. Merawa and M. Rerat, J. Chem. Phys. **106**, 3658 (1997).
[41] M. Marinescu, Phys. Rev. A **56**, 4764 (1997).
[42] S. Geltman, J. Phys. B **21**, L735 (1988).
[43] D. R. Bates and A. Damgaard, Philos. Trans. R. Soc. London, Ser. A **242**, 101 (1949).
[44] C. F. Froese-Fisher, P. Jönsson, and M. Godefroid, Phys. Rev. A **57**, 1753 (1998).
[45] V. D. Ovsyannikov, Opt. Spektrosk **53**, 600 (1982) [Opt. Spectrosc. **53**, 357 (1982)].
[46] A. I. Voronin and S. Ya. Umansky, Theor. Chim. Acta **12**, 166 (1968).
[47] S. Geltman, J. Phys. B **22**, 2049 (1989).